Clinical Radiology (2008) 63, 774–782

Diffusion-weighted magnetic resonance imaging: a potential non-invasive marker of tumour aggressiveness in localized prostate cancer

N.M. deSouza[a,*], S.F. Riches[a], N.J. VanAs[b], V.A. Morgan[a], S.A. Ashley[c], C. Fisher[d], G.S. Payne[a], C. Parker[b]

[a]*Institute of Cancer Research and Royal Marsden NHS Foundation Trust, UK,* [b]*Academic Urology Unit, Royal Marsden NHS Foundation Trust and Institute of Cancer Research, UK,* [c]*Department of Computing, Royal Marsden NHS Foundation Trust, Sutton, Surrey, UK, and* [d]*Department of Histopathology, Royal Marsden NHS Foundation Trust and Institute of Cancer Research, UK*

Received 20 November 2007; received in revised form 29 January 2008; accepted 6 February 2008

AIM: To evaluate diffusion-weighted magnetic resonance imaging (DW-MRI) as a marker for disease aggressiveness by comparing tumour apparent diffusion coefficients (ADCs) between patients with low- versus higher-risk localized prostate cancer.

METHOD: Forty-four consecutive patients classified as low- [$n = 26$, stageT1/T2a, Gleason score ≤ 6, prostate-specific antigen (PSA) < 10 (group 1)] or intermediate/high- [$n = 18$, stage $\geq$ T2b and/or Gleason score ≥ 7, and/or PSA > 10 (group 2)] risk, who subsequently were monitored with active surveillance or started neoadjuvant hormone and radiotherapy, respectively, underwent endorectal MRI. T2-weighted (T2W) and DW images (5 b values, 0–800 s/mm^2) were acquired and isotropic ADC maps generated. Regions of interest (ROIs) on T2W axial images [around whole prostate, central gland (CG), and tumour] were transferred to ADC maps. Tumour, CG, and peripheral zone (PZ = whole prostate minus CG and tumour) ADCs (fast component from b = 0–100 s/mm^2, slow component from b = 100–800 s/mm^2) were compared.

RESULTS: T2W-defined tumour volume medians, and quartiles were 1.2 cm^3, 0.7 and 3.3 cm^3 (group 1); and 6 cm^3, 1.3 and 16.5 cm^3 (group 2). There were significant differences in both ADC_{fast} ($1778 \pm 264 \times 10^{-6}$ versus $1583 \pm 283 \times 10^{-6}$ mm^2/s, $p = 0.03$) and ADC_{slow} ($1379 \pm 321 \times 10^{-6}$ versus $1196 \pm 158 \times 10^{-6}$ mm^2/s, $p = 0.001$) between groups. Tumour volume ($p = 0.002$) and ADC_{slow} ($p = 0.005$) were significant differentiators of risk group.

CONCLUSION: Significant differences in tumour ADCs exist between patients with low-risk, and those with higher-risk localized prostate cancer. DW-MRI merits further study with respect to clinical outcomes.

Introduction

Treatment options for localized prostate cancer are many and varied, ranging from immediate radical surgery through to watchful waiting (intervening only if symptoms develop). Radical prostatectomy has been shown in a good-quality, randomized, controlled trial to have an overall survival advantage compared with watchful waiting.[1] Conversely, prostate cancer can often behave in an indolent fashion even without treatment, with no effect either on health or longevity.[2] In such cases, radical treatment, with its risks of incontinence and impotence, could be worse than the disease. So, the challenge of managing localized prostate cancer is to distinguish patients with clinically relevant cancers, who may benefit from radical treatment, from the remainder who do not need any intervention. There is a major unmet need for markers of prostate cancer behaviour

* Guarantor and correspondent: N.M. deSouza, MRI Unit, Institute of Cancer Research and Royal Marsden Hospital, Downs Road, Sutton, Surrey SM2 5PT, UK. Tel.: +44 20 8661 3119/3289; fax: +44 20 8661 0846.

E-mail address: nandita.desouza@icr.ac.uk (N.M. deSouza).

0009-9260/$ - see front matter © 2008 The Royal College of Radiologists. Published by Elsevier Ltd. All rights reserved.
doi:10.1016/j.crad.2008.02.001

that could be used to support the decision whether or not to offer patients radical treatment.

A conventional approach is to classify cases into risk groups in terms of serum prostate specific antigen (PSA) level, biopsy Gleason score, and clinical T stage,[3–5] and nomograms to risk-stratify patients based on such parameters have been derived.[6,7] These risk groups have been shown to predict the probability of biochemical recurrence after radical treatment, and are used as a guide to treatment decision-making. In particular, patients with intermediate and high-risk localized prostate cancer are typically considered good candidates for immediate radical treatment with surgery or external beam radiotherapy as there is a clear survival benefit.[1] Patients with low-risk localized disease are typically offered the option of either immediate radical treatment or active surveillance. However, histological evaluation at biopsy requires an invasive procedure and is subject to sampling error. There remains a pressing need for non-invasive markers of prostate cancer behaviour, that can be applied to individual cases at the outset, to identify those requiring treatment, and those who should be monitored in an active surveillance programme with PSA and repeat biopsy.

The best method of imaging prostate cancer is with endorectal T2-weighted (T2W) magnetic resonance imaging (MRI). Unfortunately the sensitivity of T2W MRI alone varies from 60–82%, for disease detection within the gland with a specificity of around 55–70%.[8–10] Awareness of clinical data significantly improves reader detection of prostate cancer nodules with endorectal MRI, but there is no overall change in reader accuracy, because of an associated increase in false-positive findings.[11] MR spectroscopy has also been used as an adjunct to imaging and improves accuracy of prostate cancer detection,[12–15] but is time-consuming both for image acquisition and subsequent data processing and is not easy to implement in many centres. The production of citrate is reduced in cancer tissue, whereas choline is increased, leading to an increased choline to citrate ratio. An attempt to correlate MR spectroscopy with tumour aggressiveness showed that there was a trend toward increasing (choline + creatine)/citrate with increasing Gleason score, but that there was significant overlap between MR spectroscopic imaging parameters at various Gleason grade levels.[16] More recently, dynamic contrast-enhanced MRI has been investigated as a diagnostic tool for prostate cancer detection ,[17,18] but although the technique is promising, controversies exist around standardization of analysis and reporting. Thus, although MRI is useful in disease staging,[19] functional MR indices to date have not been used for predicting disease outcome in prostate cancer.

An alternative to conventional T2W MRI is to develop image contrast through ''apparent diffusivity'' (tissue water incoherent displacement over distances of 1–20 μm). Diffusion-weighted (DW) MRI been used in both clinical and research settings for detecting cerebral,[20–23] as well as cancer-related disease.[24–28] In prostate cancer, DW-MRI is proving useful in tumour detection.[29] The apparent diffusion coefficients (ADCs) derived provide quantitative information on the degree of restriction of water diffusion within tissues, including the contribution from microcapillary perfusion and Brownian diffusion within the extracellular space. Therefore, ADCs are directly associated with coherent microvessel density and cellularity[30] with microcapillary perfusion contributing to a ''fast'' diffusion component and extra- and intracellular water movement over a shorter diffusion path length contributing to a ''slow'' component.

The purpose of this study was to compare tumour ADC values between patients with clinically localized prostate cancer classified as low-risk versus those classified as intermediate or high-risk of progression, in order to determine the potential value of DW-MRI as a non-invasive marker of disease aggressiveness.

Methods

Patient population

This was a prospective, single-institution study with approval from the local research ethics committee. Over a 6-month period (July–Dec 2006), 44 consecutive patients with clinically localized prostate cancer (on digital rectal examination) referred for routine clinical evaluation in our MRI centre underwent DW-MRI in addition to their standard T2W MRI. Areas of T2W abnormality validated by biopsy results were used as positive evidence of tumour.

The patients were classified into two groups according to their risk category, defined using the NCCN criteria. Patients with low-risk localized disease (T1/T2a, Gleason score < 7 and PSA < 10) formed group 1. Patients with intermediate or high-risk disease (either $\geq$T2b and/or Gleason score ≥ 7, and/or PSA > 10) formed group 2. MRI was done at a median of 13 weeks (lower and upper quartiles 8.8 and 26.3 weeks) from the most recent biopsy. A minimum of six biopsies (apex,

mid-gland, and base from each side) were obtained in each case (14 patients had eight biopsies and 23 had 12). Patient characteristics are summarized in Table 1. Following MRI, patients were treated as indicated clinically and were either watched under an active surveillance protocol or received neoadjuvant hormonal therapy followed by radiotherapy.

Imaging methods

MRI studies were performed using a 1.5 T Intera (Philips Medical Systems, Best, the Netherlands) using a balloon-design endorectal coil (Philips Medical Systems) inflated with 55 ml air. Hyoscine butylbromide (20 mg) was administered intramuscularly immediately prior to centring the patient in the machine in order to reduce peristalsis: this is routine at our institution for abdomino-pelvic MRI and is preferred to glucagon because of more effective antiperistalsis. None of our patients had a previous history of urinary retention. Although it is contraindicated in patients with large prostates and urinary retention, given intramuscularly at this dose, there have been no cases of urinary retention in our clinical practice over the last 10 years. Conventional T2W fast spin-echo images were obtained in three orthogonal planes [TSE repetition time (TR) 2000 ms/echo time (TE) 90 ms, echo train length 16, two signal averages] with a 256×512 matrix (interpolated to 512×512), 3 mm section thickness, no gap, and a 14 cm field of view (FOV; total imaging time 12 min). Echo-planar DW images (2500/69 [TR/TE]) with b values of 0, 100, 300, 500 and 800 s/mm^2 were obtained transverse to the prostate and parallel to the corresponding set of T2W images. The phase-encoding gradient was from left to right in order to minimize motion artefacts in the prostate. Twelve 4 mm thick sections (no gap, 20 cm FOV, matrix 128×128) provided coverage of the prostate with an image acquisition time of 1 min 24 s.

Table 1 Patient characteristics for each of the groups

	Group 1	Group 2
Age (mean ± SD)	64.8 ± 6.8 years	69.4 ± 5.6 years
Stage		
T1	22	8
T2a	4	
T2b		5
T3		5
Prostate-specific antigen	5.7 + 2.4 ng/ml	18.1 + 16.8 ng/ml
Gleason score 6	26	1
Gleason score 7	–	12
Gleason score 8–10	–	5

Data analysis

The axial T2W and DW images were transferred offline for analysis. Regions of interest (ROIs) were drawn on all sections of the T2W axial images around the whole prostate, the central gland (CG), and the tumour. The tumour region was identified as a focal low signal intensity lesion or a homogeneous low-signal intensity lesion with mass-effect on the T2W images in a sextant that was biopsy positive for tumour by a radiologist with 10 years experience of prostate MRI. The radiologist had knowledge of the biopsy findings, but did not have access to the DW data and ADC maps. T2W defined tumour volumes were calculated by multiplying total tumour ROI area by the section thickness.

Software written in-house (IDL, ITT-IVS, Colorado, USA) was used to generate isotropic ADC maps over the whole range of b values (0–800 s/mm^2, $ADC_{overall}$), which reflects both perfusion and diffusion components, for b = 0–100 s/mm^2 to reflect the ''fast'' diffusion component, ADC_{fast}, and over the range b = 100–800 s/mm^2 to reflect the ''slow'' diffusion component ADC_{slow}. Manufacturer's software that automatically generates such data was not available on the MRI machine at the time. The data were fitted with a single exponential in each case. The centre of mass and whole gland outlines defined on ADC maps were matched with those defined on the T2W images to correct for rigid body shifts.[31] T2W ROIs were transferred onto the corresponding sections on the ADC maps. Mean ADC values from tumour, CG, and non-malignant peripheral zone (PZ, whole prostate minus CG and tumour) were calculated.

Statistical analysis

The data were tested for normality using a Shapiro–Francia test. The distribution of values for MR-defined tumour volume and for $ADC_{overall}$ were found to be non-normal. These data were, therefore, log transformed and the log-transformed data tested for normality. All other data were normally distributed. A paired *t*-test to assess within-group differences (between tumour, CG and PZ in the same prostate) and an independent samples *t*-test with Bonferroni correction to assess differences between means of the two groups were used. Differences in $ADC_{overall}$, ADC_{fast}, and ADC_{slow} between tumour ROIs, CG, and non-malignant PZ were calculated and a *p*-value of <0.05 was taken to be significant. A logistic regression model was used to determine parameters predictive of risk, and a receiver operating characteristic (ROC) curve was subsequently plotted to determine the cut-off value for this parameter.

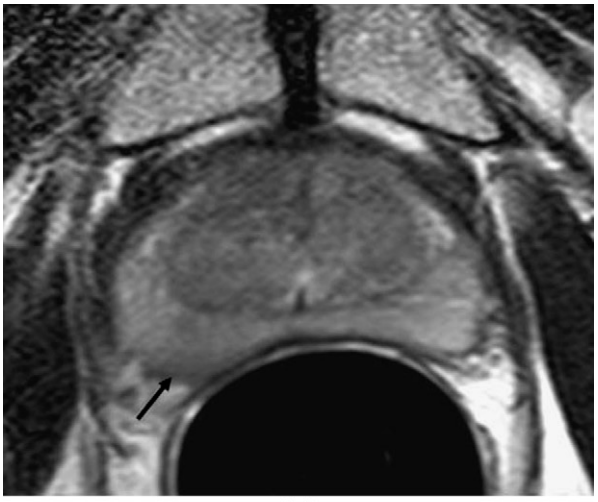

(a)

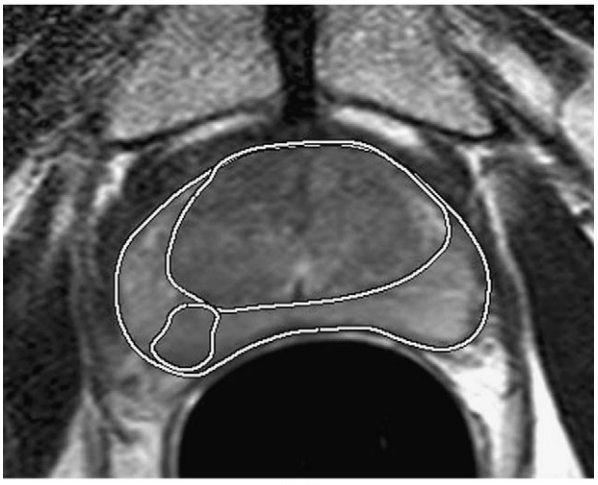

(b)

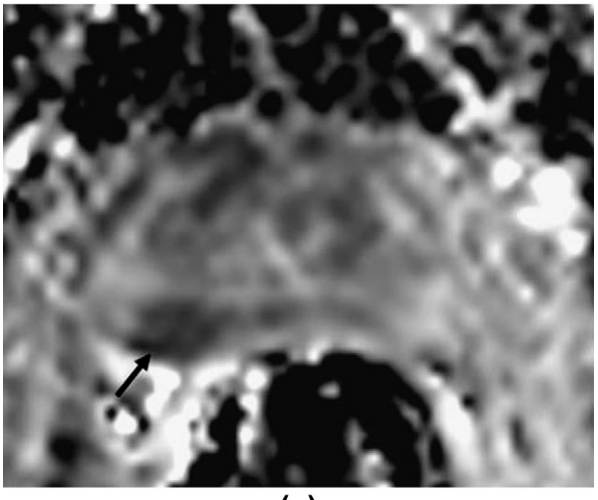

(c)

Figure 1 Patient with low-risk prostate cancer. Endorectal T2W transverse image (a) shows a well-defined low signal intensity region in the peripheral zone on the right (arrow), within a sextant that was biopsy positive for tumour. A radiologist-determined region of interest around the tumour, whole prostate and CG are shown in (b). An ADC map (c) shows the restricted diffusion in the right peripheral zone posteriorly (arrow).

Results

Group 1

Thirty-six tumour lesions were identified in 26 patients. These were identified as low-signal-intensity lesions in the PZ (Fig. 1a and b) or irregular, homogeneous, low signal intensity lesions in the CG with mass effect. The size, margins, and mass effect of the CG lesions were in keeping with tumour[32] as opposed to fibromuscular nodules of benign prostatic hypertrophy. All the corresponding sextants were biopsy positive for tumour. Eight of these lesions were relatively subtle and required review of the T2W MRI after taking the biopsy findings into consideration. In the other 28 lesions, the lesion was easily discernible on the T2W images, and the biopsy findings were used as confirmatory evidence. In patients with more than one tumour focus, a single tumour ADC was calculated from all tumour voxels. Tumour ROI volume ranged from 0.15—12.6 cm^3 (mean 2.3 ± 2.8 cm^3, median 1.2 cm^3, quartiles 0.68, 3.3 cm^3). One sextant in one patient was biopsy positive with no corresponding T2W abnormality, and therefore, was not included as a tumour ROI in the analysis. Comparison of ADC values in lesions <1 cm^3 ($n = 10$) with those from lesions ≥ 1 cm^3 ($n = 16$) showed no significant difference between the means ($p = 0.09$), indicating that partial volume effects in smaller tumours are unlikely to affect the group mean ADC values.

Group 2

Twenty-three tumour lesions were identified in 17 patients (Fig. 2a and b). All these lesions were easily identifiable on T2W MRI as a low signal-intensity mass with a biopsy from a corresponding sextant of the prostate positive for tumour. In patients with more than one tumour focus, a single tumour ADC was calculated from all tumour voxels. Tumour ROI volume ranged from 0.3—132.9 cm^3 (mean 15.7 ± 30.5 cm^3, median 6 cm^3, quartiles 1.3, 16.5 cm^3). Two sextants in one patient were biopsy positive with no corresponding T2W abnormality and this region, therefore, was not included as a tumour ROI in the analysis.

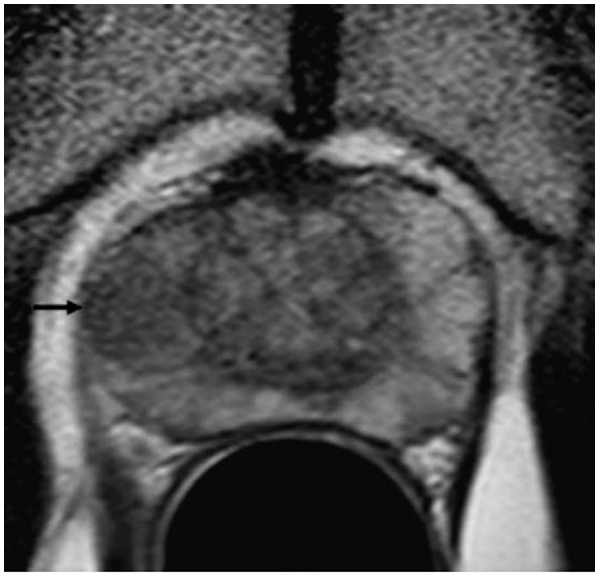

(a)

(b)

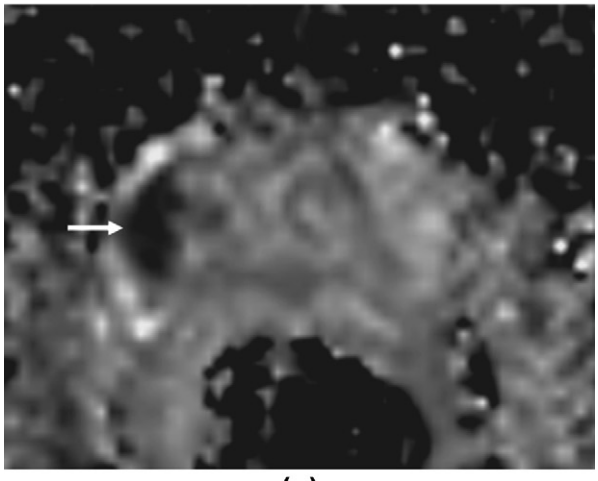

(c)

Comparison between low- and high-risk groups

Heterogeneity of ADC was observed within tumour ROIs in all cases (Figs. 1c and 2c). Isotropic ADC values averaged over the ROI are given in Table 2 for regions of tumour, PZ, and CG. For tumour ROIs, there was a significant difference between the two groups in both the ADC_{fast} ($b = 0-100$ s/mm^2) and ADC_{slow} ($b = 100-800$ s/mm^2) components (Table 2). The PZ and CG values did not show any significant differences between groups. There also was a significant difference in both the ADC_{fast} and ADC_{slow} components between tumour and PZ ($p = 0.0001$), and between PZ and CG ($p = 0.0001$) in both groups, and between tumour and CG ($p = 0.0001$) for group 2, but not group 1 ($p = 0.053$).

Predictors of disease aggressiveness

ADC_{fast} ($p = 0.013$) and ADC_{slow} ($p = 0.005$) were discriminatory between risk groups. T2W defined tumour volume was also a significant predictor of risk group ($p = 0.002$). Logistic regression showed that ADC_{slow} enabled correct prediction of risk group 72.7% of the time (area under ROC curve, AUC = 0.76), whereas the log MR-defined tumour volume enabled correct prediction of risk group 79.7% of the time (AUC = 0.76; Table 3). However, with the relatively small numbers of patients in this study, these parameters failed to show independent significance. For a 70% accuracy of risk prediction, using a tumour ADC_{slow} cut-off of 1333×10^{-6} mm^2/s gave a sensitivity of 89% and specificity of 58%, whereas a cut-off of 1200×10^{-6} mm^2/s, gave a sensitivity of 55% and specificity 95%. Also, for a 77% accuracy of risk prediction using tumour volume, a cut-off of 3.75 cm^3 gave a sensitivity of 61% and specificity of 88%.

Discussion

This study demonstrates that the slow and fast components of water diffusion within prostate tumours are significantly different in patients with

Figure 2 Patient with high-risk prostate cancer. Endorectal T2W transverse image (a) shows a well-defined low signal intensity region in the peripheral zone on the right (arrow), within a sextant that was biopsy positive for tumour. A radiologist-determined region of interest around the tumour, whole prostate and CG are shown in (b). An ADC map (c) shows the restricted diffusion in the right peripheral zone laterally (arrow).

Table 2 Calculated mean and standard deviation apparent diffusion coefficient (ADC) values in group 1 (low risk) and group 2 (intermediate/high risk)

	ADC tumour ($\times 10^{-6}$ mm^2/s)			ADC PZ ($\times 10^{-6}$ mm^2/s)			ADC CG ($\times 10^{-6}$ mm^2/s)		
B-values	0–800	0–100	100–800	0–800	0–100	100–800	0–800	0–100	100–800
	$ADC_{overall}$	ADC_{fast}	ADC_{slow}	$ADC_{overall}$	ADC_{fast}	ADC_{slow}	$ADC_{overall}$	ADC_{fast}	ADC_{slow}
Low-risk ($n = 26$)	1656 ± 322	1778 ± 264	1379 ± 221	2192 ± 237	2111 ± 146	1598 ± 129	1770 ± 179	1887 ± 157	1441 ± 95
High-risk ($n = 18$)	1501 ± 256	1583 ± 213	1196 ± 158	2045 ± 307	2018 ± 205	1535 ± 213	1744 ± 159	1844 ± 162	1441 ± 140
p-Value	0.24	0.03	0.001	0.24	0.24	0.66	1.0	1.0	1.0

The *p*-values relate to the differences in apparent diffusion coefficient (ADC) values between the groups. CG, central gland; PZ, whole prostate minus CG.

low-risk compared with those with intermediate or high-risk disease. ADC values thus offer potential for differentiating indolent from aggressive prostate cancers. Water diffusion characteristics are substantially affected by cellular and structural changes within tissues because this parameter is strongly affected by cell density, vascularity, viscosity of extracellular fluid, membrane permeability between intra- and extracellular compartments, active transport and flow, and directionality of tissue/cellular structures that impede water mobility. This study, therefore, confirms that these cellular and structural differences exist between low and high-risk lesions, and that they can be measured non-invasively *in vivo*. Although ADC values are known to correlate with tissue structure, the NCCN criteria rather than Gleason score were used to define risk groups in order to reduce the effects of biopsy sampling variability and reflect the fact that our ADC values were averaged over the whole tumour ROI. Averaging ADCs over the ROI is a limitation as it does not account for ADC differences within the tumour itself: correlation of these differences with histopathology would be useful. Further study of DW-MRI in localized prostate cancer is also warranted in relation to histopathological and clinical outcomes.

The methodology used in the present study enables calculation of diffusion components weighted to low and high b values. Although some researchers have advocated the use of b values of 1000 s/mm^2 in order to separate out the slow diffusion components adequately, our data shows that values up to 800 s/mm^2 are sufficient: use of higher b values merely serves to increase the noise in the acquired data. *Ex vivo* data show that it is the slow diffusion component that is associated with cell density.[33] Thus the ADC_{slow} differences between high and low-risk groups may be due to highly cellular regions in high-risk patients. However, it does not explain why the fast diffusing component traditionally linked with capillary microcirculation should be diminished in the high-risk group. It is possible that microcapillary perfusion is compromised in the high-risk patients because of tumour hypoxia. This is supported by *ex vivo* findings of increased hypoxia in more aggressive tumour types.[34]

Table 3 Slow component of apparent diffusion coefficients (ADC) as a predictor of risk group

Observed		Predicted ADC_{slow}		
		Risk group		% correct
		Low risk	High risk	
Risk group	Group 1	22	4	84.6
	Group 2	8	10	55.6
Overall percentage				72.7

As T2W low signal intensity lesions are well described not only in cancer, but also in infection, inflammation, and fibrosis, the likelihood of these lesions contributing to our ROIs were reduced by including only T2W lesions that had a positive sextant biopsy. Sextant biopsies were used as the minimum, although it is acknowledged that a larger number of biopsies improves disease detection.[35] It is well recognized that biopsies are subject to sampling error, and T2W hypointensity can represent chronic prostatitis rather than tumour. Although a thorough correlation was attempted, it is possible that in group 1 DW abnormalities did not correspond to tumour foci. In group 2, where tumour volume was large, sampling error is much less likely. Evidence of high signal intensity was investigated for within these regions on the T1W images of the whole pelvis taken at the same time to indicate haemorrhage, as this would have affected the ADC measurement. The quantitation of ADC served to eliminate signal variations due to receiver gain and surface coil signal inhomogeneities.

In agreement with previous findings, prostate cancer has a lower ADC value than non-malignant

peripheral zone.[31,36,37] In comparison, ADC values of tumours have previously been described as indistinguishable from the CG where hypercellular BPH nodules may have low ADCs.[36] We have shown that it is possible to distinguish ADCs in tumours from those in the CG in high-risk patients. This could be of benefit in identifying those with CG tumours that require treatment. The main clinical value would be to identify adverse disease on DW-MRI that was considered low-risk according to established clinical characteristics. However, if a patient is thought to have high-risk disease on the basis of T stage, Gleason score, and PSA, then management unlikely to be influenced by favourable DW-MRI results. DW-MRI has also been shown to be significantly better than T2W MRI at field strengths of 3 T,[38] and further benefits are seen when used in combination with dynamic contrast-enhanced imaging.[39]

In prostate cancer, tumour volume is recognized as an important predictor of clinical stage and disease outcome: in a multivariate analysis, tumour volume was an independent predictor of PSA recurrence ($p = 0.04$).[40] In one large study, significant correlations between tumour volume and known prognostic parameters, such as preoperative serum levels of PSA, loss of differentiation, histological grade, lymph node metastasis, and margins were found.[41] However, in practice, clinicians place little emphasis on tumour volumes, as reliable measures of tumour volume are not readily available. Estimates of tumour volume derived from radical prostatectomy have been shown to correlate with volumes on T2W MRI,[42] although in some studies[43] and in tumours less than 1 cm in diameter, the correlation with tumour size at histology is much poorer.[44] In this study, tumour volume was significantly higher in group 2 and confirms the value of both T2W-defined tumour volume and the slow component of ADC in differentiating low from high-risk groups.

There is a major unmet need for markers of prostate cancer behaviour, especially within the low-risk group, and it is in this group of patients where the additional information provided by DW-MRI is likely to be most beneficial. This group of patients are faced with the difficult decision of whether or not to have radical treatment, needing to weigh up the potential survival benefit against the known morbidity. Active surveillance is an approach to the management of localized prostate cancer that aims to avoid over treatment of men with indolent cancers, while still providing treatment with radical intent within a window of curability for those who need it. Active surveillance programmes rely on PSA kinetics and repeat biopsies to risk-stratify patients and guide decisions on who needs treatment and when. Hence risk stratification relies to an extent on information obtained from needle biopsy. It is well known that sampling error is a major limitation of needle biopsies. DW-MRI provides information on the whole gland and gives biological information, which may be used in addition to, or as a non-invasive surrogate for, the prognostic information derived from biopsies. Separation of high and low-risk lesions has also been described using MRS, which is the only other functional imaging technique where risk stratification has been attempted according to Gleason grade. In the study of Zakian et al.,[16] the AUC for separating low from high-risk lesions using the maximum Cho + Cr/Cit was 0.8, with overlap between MRS parameters at various Gleason scores. Tumour volume was also found to correlate with Gleason score. Investigation of a combination of the slow component of ADC, MRS and tumour volume as a tool in the management of localized prostate cancer is, therefore, warranted.

A major limitation of this study is the lack of correlation of tumour ROIs with whole mount histopathology. However, our clinical practice is such that these patients largely elect to remain within an active surveillance programme, or in the case of higher-risk disease undergo hormone down-regulation and radiotherapy. In the high-risk cohort, all lesions were large and easily discernible on T2W imaging, so the likelihood of error in ROI placement is low. In the low-risk cohort, where eight lesions were difficult to identify without the biopsy data, the ADC values are likely to have been indistinguishable from adjacent non-malignant PZ or CG. In these cases, the lack of a visually identifiable lesion on the ADC map is also an indicator of the low-risk nature of the lesion. A more problematic feature is that we used the averaged ADC from the entire tumour region, and this was often heterogeneous. It may be that the more restricted areas of diffusion within the tumour region are ultimately more predictive of outcome.

In conclusion, DW-MRI offers potential as a non-invasive marker of biologically aggressive cancer. Tumour volume and the slow diffusion component appear to be discriminators of higher-risk disease. DW-MRI is simple to implement and the time penalty when added to a standard endorectal staging MRI examination is less than 2 min. However, further work is needed to determine the best cut-off values of ADC. There is a need also to establish the potential of DW-MRI in longitudinal studies in patients on active surveillance in order to determine when to implement treatment.

Acknowledgements

This study was supported by Cancer Research UK (grant number CUK C1060/A808).

References

1. Bill-Axelson A, Holmberg L, Ruutu M, et al. Radical prostatectomy versus watchful waiting in early prostate cancer. *N Engl J Med* 2005;**352**:1977–84.
2. Albertsen PC, Hanley JA, Gleason DF, et al. Competing risk analysis of men aged 55 to 74 years at diagnosis managed conservatively for clinically localized prostate cancer. *JAMA* 1998;**280**:975–80.
3. Chism DB, Hanlon AL, Horwitz EM, et al. A comparison of the single and double factor high-risk models for risk assignment of prostate cancer treated with 3D conformal radiotherapy. *Int J Radiat Oncol Biol Phys* 2004;**59**:380–5.
4. D'Amico AV, Whittington R, Malkowicz SB, et al. Biochemical outcome after radical prostatectomy, external beam radiation therapy, or interstitial radiation therapy for clinically localized prostate cancer. *JAMA* 1998;**280**:969–74.
5. Zelefsky MJ, Lyass O, Fuks Z, et al. Predictors of improved outcome for patients with localized prostate cancer treated with neoadjuvant androgen ablation therapy and three-dimensional conformal radiotherapy. *J Clin Oncol* 1998;**16**:3380–5.
6. Partin AW, Mangold LA, Lamm DM, et al. Contemporary update of prostate cancer staging nomograms (Partin Tables) for the new millennium. *Urology* 2001;**58**:843–8.
7. Stephenson AJ, Scardino PT, Eastham JA, et al. Preoperative nomogram predicting the 10-year probability of prostate cancer recurrence after radical prostatectomy. *J Natl Cancer Inst* 2006;**98**:715–7.
8. Casciani E, Polettini E, Bertini L, et al. Prostate cancer: evaluation with endorectal MR imaging and three-dimensional proton MR spectroscopic imaging. *Radiol Med (Torino)* 2004;**108**:530–41.
9. Kirkham AP, Emberton M, Allen C. How good is MRI at detecting and characterising cancer within the prostate? *Eur Urol* 2006;**50**:1163–74.
10. Graser A, Heuck A, Sommer B, et al. Per-sextant localization and staging of prostate cancer: correlation of imaging findings with whole-mount step section histopathology. *AJR Am J Roentgenol* 2007;**188**:84–90.
11. Dhingsa R, Qayyum A, Coakley FV, et al. Prostate cancer localization with endorectal MR imaging and MR spectroscopic imaging: effect of clinical data on reader accuracy. *Radiology* 2004;**230**:215–20.
12. Futterer JJ, Scheenen TW, Heijmink SW, et al. Standardized threshold approach using three-dimensional proton magnetic resonance spectroscopic imaging in prostate cancer localization of the entire prostate. *Invest Radiol* 2007;**42**:116–22.
13. Katz S, Rosen M. MR imaging and MR spectroscopy in prostate cancer management. *Radiol Clin North Am* 2006; **44**:723–34. viii.
14. Wang L, Hricak H, Kattan MW, et al. Prediction of organ-confined prostate cancer: incremental value of MR imaging and MR spectroscopic imaging to staging nomograms. *Radiology* 2006;**238**:597–603.
15. Coakley FV, Qayyum A, Kurhanewicz J. Magnetic resonance imaging and spectroscopic imaging of prostate cancer. *J Urol* 2003;**170**:S69–76.
16. Zakian KL, Sircar K, Hricak H, et al. Correlation of proton MR spectroscopic imaging with gleason score based on step-section pathologic analysis after radical prostatectomy. *Radiology* 2005;**234**:804–14.
17. Futterer JJ, Heijmink SW, Scheenen TW, et al. Prostate cancer localization with dynamic contrast-enhanced MR imaging and proton MR spectroscopic imaging. *Radiology* 2006;**241**:449–58.
18. Girouin N, Mege-Lechevallier F, Tonina SA, et al. Prostate dynamic contrast-enhanced MRI with simple visual diagnostic criteria: is it reasonable? *Eur Radiol* 2007;**17**:1498–509.
19. Jackson AS, Parker CC, Norman AR, et al. Tumour staging using magnetic resonance imaging in clinically localised prostate cancer: relationship to biochemical outcome after neo-adjuvant androgen deprivation and radical radiotherapy. *Clin Oncol* 2005;**17**:167–71.
20. Beaulieu C, D'Arceuil H, Hedehus M, et al. Diffusion-weighted magnetic resonance imaging: theory and potential applications to child neurology. *Semin Pediatr Neurol* 1999;**6**:87–100.
21. Provenzale JM, Sorensen AG. Diffusion-weighted MR imaging in acute stroke: theoretic considerations and clinical applications. *AJR Am J Roentgenol* 1999;**173**:1459–67.
22. Rowley HA, Grant PE, Roberts TP. Diffusion MR imaging. Theory and applications. *Neuroimaging Clin N Am* 1999;**9**: 343–61.
23. Sotak CH. New NMR measurements in epilepsy. Diffusion-weighted magnetic resonance imaging of spreading depression. *Adv Neurol* 1999;**79**:925–9.
24. Chenevert TL, Stegman LD, Taylor JM, et al. Diffusion magnetic resonance imaging: an early surrogate marker of therapeutic efficacy in brain tumors. *J Natl Cancer Inst* 2000;**92**:2029–36.
25. Galons JP, Altbach MI, Paine-Murrieta GD, et al. Early increases in breast tumor xenograft water mobility in response to paclitaxel therapy detected by non-invasive diffusion magnetic resonance imaging. *Neoplasia* 1999;**1**:113–7.
26. Gibbs P, Tozer DJ, Liney GP, et al. Comparison of quantitative T2 mapping and diffusion-weighted imaging in the normal and pathologic prostate. *Magn Reson Med* 2001;**46**: 1054–8.
27. Gupta RK, Cloughesy TF, Sinha U, et al. Relationships between choline magnetic resonance spectroscopy, apparent diffusion coefficient and quantitative histopathology in human glioma. *J Neurooncol* 2000;**50**:215–26.
28. Maier CF, Paran Y, Bendel P, et al. Quantitative diffusion imaging in implanted human breast tumors. *Magn Reson Med* 1997;**37**:576–81.
29. Shimofusa R, Fujimoto H, Akamata H, et al. Diffusion-weighted imaging of prostate cancer. *J Comput Assist Tomogr* 2005;**29**:149–53.
30. Hayashida Y, Hirai T, Morishita S, et al. Diffusion-weighted imaging of metastatic brain tumors: comparison with histologic type and tumor cellularity. *AJNR Am J Neuroradiol* 2006;**27**:1419–25.
31. deSouza NM, Reinsberg SA, Scurr ED, et al. Magnetic resonance imaging in prostate cancer: value of apparent diffusion coefficients for identifying malignant nodules. *Br J Radiol* 2007;**80**:90–5.
32. Akin O, Sala E, Moskowitz CS, et al. Transition zone prostate cancers: features, detection, localization, and staging at endorectal MR imaging. *Radiology* 2006;**239**:784–92.
33. Valonen PK, Lehtimaki KK, Vaisanen TH, et al. Water diffusion in a rat glioma during ganciclovir–thymidine kinase gene therapy-induced programmed cell death *in vivo*: correlation with cell density. *J Magn Reson Imaging* 2004; **19**:389–96.

34. Zhao D, Ran S, Constantinescu A, et al. Tumor oxygen dynamics: correlation of in vivo MRI with histological findings. *Neoplasia* 2003;**5**:308—18.
35. Master VA, Chi T, Simko JP, et al. The independent impact of extended pattern biopsy on prostate cancer stage migration. *J Urol* 2005;**174**:1789—93.
36. Issa B. *In vivo* measurement of the apparent diffusion coefficient in normal and malignant prostatic tissues using echo-planar imaging. *J Magn Reson Imaging* 2002;**16**: 196—200.
37. Reinsberg SA, Payne GS, Riches SF, et al. Combined use of diffusion-weighted MRI and 1H MR spectroscopy to increase accuracy in prostate cancer detection. *AJR Am J Roentgenol* 2007;**188**:91—8.
38. Miao H, Fukatsu H, Ishigaki T. Prostate cancer detection with 3-T MRI: comparison of diffusion-weighted and T2-weighted imaging. *Eur J Radiol* 2007;**61**:297—302.
39. Kozlowski P, Chang SD, Jones EC, et al. Combined diffusion-weighted and dynamic contrast-enhanced MRI for prostate cancer diagnosis—correlation with biopsy and histopathology. *J Magn Reson Imaging* 2006;**24**:108—13.
40. Nelson BA, Shappell SB, Chang SS, et al. Tumour volume is an independent predictor of prostate-specific antigen recurrence in patients undergoing radical prostatectomy for clinically localized prostate cancer. *BJU Int* 2006;**97**:1169—72.
41. Bettendorf O, Oberpenning F, Kopke T, et al. Implementation of a map in radical prostatectomy specimen allows visual estimation of tumor volume. *Eur J Surg Oncol* 2007; **33**:352—7.
42. Ponchietti R, Di Loro F, Fanfani A, et al. Estimation of prostate cancer volume by endorectal coil magnetic resonance imaging vs. pathologic volume. *Eur Urol* 1999;**35**:32—5.
43. Jager GJ, Ruijter ET, van de Kaa CA, et al. Local staging of prostate cancer with endorectal MR imaging: correlation with histopathology. *AJR Am J Roentgenol* 1996;**166**:845—52.
44. Nakashima J, Tanimoto A, Imai Y, et al. Endorectal MRI for prediction of tumor site, tumor size, and local extension of prostate cancer. *Urology* 2004;**64**:101—5.